arXiv:astro-ph/0103331v1 21 Mar 2001

ROSAT and BeppoSAX evidence of soft X–ray excess emission in the Shapley supercluster: A3571, A3558, A3560 and A3562

Massimiliano Bonamente [1], Richard Lieu [2], Jukka Nevalainen [3] and Jelle S. Kaastra [4]

[1]Osservatorio Astrofisico di Catania, Via S. Sofia 78, I-95125 Catania, Italy

[3]Department of Physics, University of Alabama, Huntsville, AL 35899, U.S.A.

[2]Astrophysics Division, ESA, ESTEC, Postbus 299, NL-2200 AG Nordwijk, The Netherlands

[4]SRON Laboratory for Space Research, Sorbonnelaan 2, 3584 CA Utrecht, The Netherlands

Received _____; accepted _____

ABSTRACT

Excess soft X–ray emission in clusters of galaxies has so far been detected for sources that lie along lines–of–sight to very low Galactic HI column density (such as Coma, A1795, A2199 and Virgo, $N_H \sim 0.9{-}2.0{\times}10^{20}$ cm^{-2}). We show that the cluster *soft excess* emission can be investigated even at higher N_H, which provides an opportunity for investigating soft X–ray emission characteristics among a large number of clusters.

The ROSAT PSPC analysis of some members of the Shapley concentration (A3571, A3558, A3560 and A3562, at $N_H \sim 4 - 4.5 \times 10^{20}$ cm^{-2}) bears evidence for excess emission in the 1/4 keV band. We were able to confirm the finding for the case of A3571 by a pointed SAX observation. Within the current sample the soft X-ray flux is again found to be consistently above the level expected from a hot virialized plasma. The data quality is however insufficient to enable a discrimination between alternative models of the excess low energy flux.

Subject headings: galaxies:clusters:individual (A3571, A3558, A3560, A3562) – intergalactic medium

1. Introduction

Clusters of galaxies are strong emitters of soft X–rays, often in excess of the contribution from the hot intra–cluster medium (ICM; Lieu at al. 1196a; Lieu et al. 1996b; Mittaz, Lieu and Lockman 1998; Lieu, Bonamente and Mittaz 1999; Bonamente, Lieu and Mittaz 2001). The PSPC detector onboard ROSAT is well suited for the observation of diffuse sources in the 1/4 keV band: along with a large effective area (of about 200 cm^2 at 0.28 keV), the large field-of-view of 1 degree radius allowed the contemporaneous acquisition of

source signals (usually near boresight) and local background (at large detector radii) with equal exposures. The Low–Energy Concentrator Spectrometer (LECS) aboard BeppoSAX also has appreciable effective areas (of ~ 10 cm^2 at 0.28 keV) and can be used for similar investigations.

Soft X–ray fluxes are significantly absorbed by intervening Galactic material (mainly HI and HeI) along the line of sight. At the Galactic N_H values of the Shapley supercluster ($\sim 4 - 4.5 \times 10^{20}$ cm^{-2}), 0.2 keV photons encounter a total optical depth of ~ 4, which accordingly reduces their flux by about 98 %. The HeI absorption cross–section was recently revised (Yan et al. 1998 and references therein), leading to a reinstatement of the original absorption code of Morrison and McCammon (1983) as the most reliable. This code is therefore employed in the present work. The crucial task, however, is to measure N_H with a spatial resolution $\leq$ the cluster size. For details on how this was fulfilled, see section 2. In this paper we present results on a sample of nearby clusters (A3571, A3558, A3560 and A3562, at redshift z$\sim$ 0.04-0.05) in the Shapley concentration. The analysis of four PSPC observations revealed statistically significant 1/4 keV band ($\sim$ 0.2–0.4 keV) excess emission for *all* of the clusters, although the intrinsic low surface brightness of A3560 and A3562 implied a limited S/N. Data from two pointed SAX/LECS observations were available for two of the four clusters (A3571 and A3562); clear evidence of soft excess emission is present in the A3571 data, while results for A3562 were marginal, due to the faintness of the cluster. Thus the soft excess syndrome may *be common to a large fraction of clusters*, as suggested also by our earlier analyses of a nearby sample of clusters with *EUVE*, contrary to the findings of Bowyer et al. (1999,2001) which claim no general importance of the effect (see also Lieu et al. 1999 and Bonamente, Lieu and Mittaz 2001 for reinforcement of the original conclusions through confirmatory re-observations conducted in such modes as to address all the objections of our critics.). This *paper* presents the data analysis method and results for the current sample, with emphasis on the PSPC analysis; future works will be

devoted to larger scale surveys, with both PSPC and LECS instruments, in order to assess the cosmological impact of the phenomenon.

2. Infrared, 21–cm and X–ray observations of A3571, A3558, A3562 and A3560

The Shapley Supercluster is a large region of galaxy overdensity around $\alpha = 13^h25^m$, $\delta = -30^o$ and redshift ~ 0.045 (Shapley 1930; Ettori, Fabian and White 1997 and references therein) comprising more than 20 galaxy clusters. We focused our attention on four Supercluster members: A3571 and A3558 are rich and hot clusters (Markevitch et al. 1998; Markevitch and Vikhlinin 1997), A3560 (Ebeling et al. 1996) and A3562 (White 2000; see also Ettori et al. 2000) are within ~ 2 degrees from the former and show lower X–ray luminosity (Fig. 1). All clusters were targets of pointed PSPC observations (archival identification code RP800287 for A3571, exp. time 5 ks; RP800076 for A3558, 28 ks; RP800381 for A3560, 5 ks; RP800237 for A3562, 18 ks), and two of them of pointed SAX LECS/MECS observation (observation number 60843002 for A3571, 29 ks of LECS exposure, and 60638001 for A3562, 19 ks) .

Dedicated narrow–beam 21–cm observations of galaxy clusters are available from the NRAO 100–meter GBT telescope [1] with a resolution of 10 arcmin (Murphy, Sembach and Lockman 2001; see Table 1). In addition we also consulted the Dickey and Lockman (1990) survey data at lower resolution and IRAS 100 μm maps with ~ 3 arcmin resolution (Wheelock et al. 1994). In particular, the IRAS data has a two–fold relevance to soft X–ray studies: on one hand the positive N_H–IR correlation allows the use of 100 μm maps

[1]The National Radio Observatory is operated by Associate Universities, Inc., under co-operative agreement with the National Science Foundation.

as tracer of the total column density of Galactic material (Boulanger and Perault 1988); on the other hand, the N_H–soft X–ray background (SXB) anticorrelation (Snowden et al. 1998) requires precise knowledge of the HI column density at the position where the local background was determined. In the case of PSPC this is typically a few × 10 arcmin away from the cluster center.

3. PSPC analysis

The analysis of PSPC data was performed following the prescriptions of Snowden et al. (1994); in particular, detector gain corrections were applied using the dedicated FTOOL PCPICOR, and detector vignetting was accounted for in the background subtraction procedure. The spectral analysis involved only PI channels 20–201 ($\sim$ 0.2–2.0 keV by photon energy), in order to avoid any calibration uncertainties of the lower energy 1–19 PI channels. Following the nomenclature reported in Snowden et al. (1994), PI channels 20-41 will be referred to as the R2 band (also 1/4 keV or C band), and channels 42–69 as R34 band.

First, we compared the IR emission of the cluster regions with the emission in the corresponding background regions (Fig. 1); deviations were always within at most 10 %, and this implies that the SXB of the background regions is indeed relevant to the cluster regions without further scaling (see Snowden et al. 1998). Secondly, a comparison of the IR emission between the cluster regions covered by the GBT beam ($\sim$ 10 arcmin angular diameter) and the outer cluster regions showed that the N_H is smoothly distributed on the cluster's scale. In accordance to the N_H–IR correlation (with a scaling factor of about 1.2 $\times 10^{20}$ cm^{-2} (MJy sr^{-1})$^{-1}$; Boulanger and Perault 1988) the 100 μm maps implied only marginal adjustments from the central N_H measurements; as a consequence, we decided to apply Galactic column densities as in Table 1 for all subsequent analyses.

The limited passband of the PSPC instrument can only be used to measure approximate values of the cluster hot gas temperatures. Thus we modelled the A3571 and A3558 spectra for annular regions with the best–fit temperatures of ASCA (Markevitch et al. 1998; Markevitch and Vikhlinin 1997; in agreement with SAX/MECS results for A3571, see Nevalainen et al. 2001), with the exception of the central regions where temperature gradients are too steep for the point spread function (PSF) of ASCA: here T was fitted to the data. Temperatures of A3560 and A3562 were determined by spectral fits to the PSPC data, and results agreed with previously published measurements (White 2000 and Ebeling et al. 1996). We modelled the entire PSPC X–ray spectrum (0.2–2.0 keV) with a one–temperature photoabsorbed thin–plasma emission code (WABS and MEKAL codes in XSPEC).

Background spectra for subtraction purposes were extracted from same pointed observation as the cluster's, and from annular regions immediately outside the detected cluster emission (see Fig. 1); statistical errors in the background were properly propagated. This provides a spatially and temporally contiguous (or *in situ*) background. Best parameter values for the hot gas are shown in Table 1. As the χ^2 values indicate, some of the fits are poor, due to the excess emission above the 1-T model at low energies. In more detail, we compared the best–fit model with the measured emission in the R2 and R34 bands (Fig. 2 and 3). The 1/4 keV band results show consistently *positive* residuals for all of the 4 clusters; the R34 band bears, on the other hand, evidence of depleted fluxes in some regions. For A3571 and A3558, there is evidence of an increasing relative importance of the excess component with cluster radius, an effect already found in EUVE data of other galaxy clusters (Virgo, A1795 and A2199; see, e.g., Bonamente, Lieu and Mittaz 2001 and Lieu, Bonamente and Mittaz 1999).

4. SAX LECS analysis

The SAX mission lends an additional view of the phenomenon, with an instrument, LECS, that employs different and complementary characteristics. With a field of view of radius $\sim$ 16 arcmin, local background can be obtained only for compact clusters (such as A3562); a long-term campaign of accumulation of high Galactic latitude 'blank' fields, however, enables one to establish a template detector background applicable to clusters which fill the entire FOV (such as A3571; see Parmar et al. 1999). The energy dependent Point Spread Function (PSF) of the LECS instruments complicates the analysis of extended objects such as clusters of galaxies, as its 90% encircled energy radius increases from $6'$ to $9'$ between 8 keV and 0.2 keV. In this work, we accounted for the PSF by generating appropriate instrument response files to be used when fitting the accumulated spectra. For the response generation we used the ray-tracing code LEMAT (Lammers 1997), taking into account the extraction region size and source position on the detector, mirror vignetting and obscuration by the detector support structure (strongback). [2]

Modeling of the low-energy emission from A3571 was performed through a joint fit of MECS/LECS spectra to a photoabsorbed MEKAL code (as for PSPC), which returned the best-fit parameters of the hot ICM consistent with those of Table 2 (see Nevalainen et al.

[2]For any given spatial region and energy range, LEMAT estimates the contribution of photons from regions external to the extraction region, and the number of photons originating from within the extraction region that are detected externally (see Kaastra et al. (1999); Nevalainen et al. (2001) for the application of LEMAT in the case of the clusters A2199 and A3571). Further applications of LEMAT to spectra of extended sources is in progress (Oosterbroek 2001); preliminary results indicate that using the LEMAT–produced responses in spectral fits of spectra obtained within a radius of 15' removes the significant instrumental distortions (except for the whole band normalization which can vary by $\pm$ 30%).

2001 for the details on the LECS/MECS analysis of this data set): excess emission in the 0.15-0.3 keV region[3] is again detected with high statistical significance (Fig. 4). The faint emission from the A3562 cluster was likewise assessed by modelling LECS spectra with the customary photoabsorbed MEKAL code, where the hot ICM parameters were fixed at the values of Table 2; results are marginalized by the lower S/N (see Fig. 4). It is worthwhile to point out that the *in situ* background, available for this cluster from an outer annulus where the source emission ceased, is fully consistent with the template 'blank' field background. This is a crucial test which verifies the reliability of the latter for those cases where the size of the cluster renders the former unavailable.

5. Interpretation of R2 and R34 band fluxes

The results shown in Fig. 2 (and Fig. 4) indicate that the 1–T model employed to describe the ICM falls short of the detected soft emission, revealing the *soft excess* emission. The data quality for A3571 and A3558 warrants the employment of a more complex model to try to interpret the detected spectral features.

The A3558 soft excess is virtually unaccompanied by a R34 trough, and therefore a

[3]At 0.28 keV, the LECS energy resolution is $\sim 32\%$ (Parmar et al. 1997), about 3 times better than PSPC's. This renders it difficult to translate PSPC pulse-invariant (PI) channels into corresponding LECS band for the purpose of comparison. Our present choice of using 0.15-0.3 keV band of LECS as *equivalent* to PSPC PI channels 20-41 is based on the 10% peak response studies of Snowden et al. (1994). Similarly, PSPC R34 band has 10 % of peak response 0.2–1.01 keV; moreover LECS data of A3571 also bear evidence of depleted fluxes around 0.5 keV (Nevalainen et al. 2001), though no attempt is made here to extract and compare such fluxes with those of the PSPC.

second optically–thin plasma component at lower temperature can model the excess. We shall present the 3–6 and 6–9 arcmin annuli as representative regions, just outside the central cooling flow, and where signals are of sufficient statistical quality to apply detailed modelling, see Table 2. We likewise tested the possiblity of the excess originating as an inverse Compton (IC) effect, with the result that the data equally well accomodates the non–thermal interpretation (see Table 2 for details). We also calculated the energetic requirements of the additional model, with the results that the luminosity of either thermal/non thermal component accounts for only a fraction of the hot ICM luminosity in the 0.1–0.4 keV band.

Moving to A3571, we again describe a representative region, the 4–8 arcmin annulus. Here the $\sim 3\sigma$ R2 band excess pairs with a depleted emission in the neighboring R34 band (Fig. 2 and 3.), i.e. the employement of a second thin plasma model at lower T brings only a modest improvement to the fit. We know, however, that warm photoionized gas (T $\sim 10^6$ K) may present substantial opacity to soft X–ray photons (e.g., Krolik and Kallman 1984), and the thin–plasma approximation may not necessarily apply. A phenomenological way of parametrizing such behaviour is the addition of a second thin–plasma model modified by an absorption edge, which in fact proves a successful fit to the data (see best–fit parameters in Table 2). Other regions of Table 2 show a qualitatively similar behavior, see Fig. 2 and 3; statistical quality of the data does not however warrant a more detailed modelling for them.

We also entertained the notion of a soft X–ray excess as peculiar variations of the Galactic N_H (Arabadjis and Bregman 1999), by applying the same 1–T thermal models above leaving the N_H to be fitted by the data. The A3571 and A3558 PSPC spectra would in such case require a Galactic column density at odds with the measured values, and some 1/4 keV band excess would nonetheless remain unexplained (see Table 1 and Fig. 5).

6. Discussion and conclusions

The analysis we present in this paper shows that, at soft X–ray energies, PSPC spectra of the clusters in our sample (A3571, A2558, A3560 and A3562) are *not* well described by a simple one–temperature thin plasma model. Similar conclusions hold for the LECS data of A3571 and A3562. The case of A3558, the cluster with the higest S/N data of the sample, indicates that the soft excess can be interpretated as having a thermal origin (from a second phase of the ICM at lower temperature) as well as the non–thermal. Earlier *EUVE* observations led to the discovery of soft excess emission for the brightest clusters with low Galactic HI columns (such as Coma and Virgo, see references in section 1), but they lack the necessary sensitivity to enable a reliable assesment of fainter sources, such as those reported in this work. The PSPC and LECS data presented here show that, given a sufficient sensitivity, low energy spectra of galaxy clusters *consistently* show excess emission above the hot ICM contribution, in sharp contrast with the conclusions of Bowyer et al. (2001). Settlement of the issue regarding the origin of the emission has to await forthcoming observations by detectors of higher resolution.

The BeppoSAX satellite is a joint Italian-Dutch programme. We thank the staff of the BeppoSAX Science Data and Operations Control Centers for help with these observations. MB and RL acknowledge the support of NASA/ADP. JN acknowledges an ESA Research Fellowship.

References

Arabadjis,J.S. and Bregman, J.N. 1999, *ApJ*, **514**, 607.

Bonamente, M., Lieu, R. and Mittaz, J.P.D. 2001, *ApJ* **547**, L7.

Bowyer, S., Berghöfer, T.W. and Korpela, E.J. 1999, *ApJ*, **526**, 592.

Bowyer, S., Korpela, E.J. and Berghöfer 2001, *ApJ*, **548** L135.

Boulanger, F. and Perault, M. 1988, *ApJ*, **330**, 964.

Dickey., J.M. and Lockman, F.J. 1990, *Ann. R. Astron. Astrop.*, **28**, 215.

Ebeling, H., Voges, W., Böringher, H., Edge, A.C., Huchra, J.P. and Briel, U.G. 1996, *MNRAS*, **281**, 799.

Ettori, S., Fabian, A.C. and White, D.A. 1997, *MNRAS*, **289**, 787.

Ettori, S., Bardelli, S., De Grandi, S., Molendi, S., Zamorani, G. and Zucca, E. 2000, *MNRAS*, **318**, 239.

Kaastra, J.S., Lieu, R., Mittaz J.P.D. et al., 1999, *ApJ*, **519**, 119.

Lammers, U. 1997, *The SAX LECS Data Analysis System - Software User Manual* , ESA/SSD, SAX/LEDA/0010.

Lieu, R., Mittaz, J.P.D., Bowyer, S., Lockman, F.J., Hwang, C.-Y. and Schmitt, J.H.H.M. 1996a, ApJ, **458**, L5.

Lieu, R., Mittaz, J.P.D., Bowyer, S., Breen, J.O., Lockman, F.J., Murphy, E.M. & Hwang, C. -Y. 1996b, *Science*, **274**,1335–1338 .

Lieu, R., Bonamente, M. and Mittaz, J.P.D. 1999, *ApJ*, **517**, L91.

Lieu, R., Ip, W.-I., Axford, W.I. and Bonamente, M. 1999, *ApJ*, **510**, L25.

Markevitch, M. et al., 1998, *ApJ*, **503**, 77.

Markevitch, M. and Vikhlinin, A., 1997, *ApJ*, **474**, 84.

Mittaz, J.P.D., Lieu, R., Lockman, F.J. 1998, *ApJ*, **498**, L17.

Morrison, R. and McCammon, D. 1983, *ApJ*, **270**, 119.

Murphy, E.M., Sembach, K.R. and Lockman, F.J. 2001, *in preparation.*

Yan, M., Sadeghpour, H.R. and Dalgarno, A. 1998, *ApJ*, **496**, 1044.

Nevalainen, J., Kaastra, J.S. and Parmar, A.N. 2001, *A & A in press.*

Oosterbroek, T. et al. 2001, *in preparation.*

Parmar, A.N. et al. 1997, *A & AS*, **122**, 309.

Parmar, A.N et al. 1999, *A & AS*, **136**, 407.

Shapley, H. 1930, *Harvard Obs. Bullettin*, **874**, 9.

Snowden, S.L., McCammon, D., Burrows, D.N. and Mendenhall, J.A. 1994, *ApJ*, **424**, 714.

Snowden, S.L., Egger, R., Finkbeiner D.P., Freyberg, M.J. and
Plucinsky, P.P. 1998, *ApJ*, **493**, 715.

Wheelock, S. et al., 1994, *IRAS Sky Survey Expl. Supp.*, (IPL Publ. 94-11), Pasadena, CA.

White, D.A. 2000, *MNRAS*, **312**, 663.

Yan, M., Sadeghpour, H.R. and Dalgarno, A. 1998, *ApJ*, **496**, 1044.

Figure captions

Figure 1: Schematic of the field of the four clusters (A3571, A3558, A3560 and A3562). Large solid circles represent the approximate cluster positions, the two small circles between A3562 and A3558 are the groups of galaxies SC1329 and A1327 (respectively from left to right; see Ettori et al. 1997 for more detailed maps). Each dotted annulus (or sector thereof) represents the approximate region from which the background for the corresponding cluster was extracted; care was taken in avoiding regions occupied by SC1329 and SC1327 and obvious point sources.

Figure 2: Radial distribution (in arcmin, x-axis) of the fractional R2 band excess, η, of the four clusters, defined as $\eta = (p_2 - q_2)/q_2$, where p_2 is observed R2 band flux and q_2 the expected R2 band flux from the hot ICM. Negative values of ζ indicate that detected emission is below the expected value.

Figure 3: As in Figure 2, except now for the fractional R34 band excess $\zeta = (p_{34} - q_{34})/q_{34}$ where p_{34} is observed R34 band flux and q_{34} is expected R34 band flux from hot ICM.

Figure 4: Radial distribution of the SAX/LECS fractional excess in the 0.15-0.3 keV band for A3571 and A3562, plotted in the same manner as Figure 2.

Figure 5: As in Figure 2, except here the expected ICM fluxes are derived by fitting N_H. Soft excess fluxes in some regions of A3571 remain nonetheless unexplained. In order to eliminate such excesses, we estimate that a N_H of $4.05\ \pm^{0.15}_{0.2} \times 10^{20}$ (4-8 arcmin region) and $3\ \pm^{0.5}_{0.4} \times 10^{20}$ (12-16 arcmin region) would be required, significantly *lower* than the measured values (see Table 1).

Tables

Table 1: Best parameters of the single temperature hot gas for the clusters in the sample. Errors are 90 % confidence level (χ^2 + 2.7 criterion); where no errors are reported, the parameters were not fitted to the data (see text). Fitted T values are obtained keeping NH fixed at the Murphy, Sembach and Lockman (2001) values. In bold-face are the N_H values from pointed observations of Murphy, Sembach and Lockman (2001); the survey values are from Dickey and Lockman (1990), with average over a 3×3 square degrees area.

Cluster	region (arcmin)	N_H	Survey N_H	best-fit N_H	T (keV)	A	χ^2 (d.o.f)
A3571	0–2 [a]	**4.4**	3.9	$3.77\ \pm^{0.47}_{0.37}$	$4.5\ \pm^{2.0}_{1.1}$	$0.6\pm^{0.61}_{0.38}$	113(139)
	2–4	”	”	$4.54\ \pm^{0.33}_{2.9}$	7	0.3	159(139)
	4–8	”	”	$4.36\ \pm^{0.36}_{0.3}$	7	0.3	233(162)
	8–12	”	”	$4.12\ \pm^{0.78}_{0.74}$	7	0.3	98(116)
	12–16	”	”	$4.25\ \pm^{3}_{1.25}$	5	0.3	110(92)
A3558	0–3	**4.0**	3.9	$3.75\ \pm^{0.21}_{0.2}$	$3.2\ \pm^{0.4}_{0.35}$	$0.33\ \pm^{0.1}_{0.1}$	209.6(179)
	3–6	**4.0**	”	$3.65\ \pm^{0.15}_{0.15}$	5	0.3	211(180)
	6–9	**4.0**	”	$3.4\ \pm^{0.17}_{0.2}$	5	0.3	237.7(176)
	9–12	4.1	”	$3.5\ \pm^{0.37}_{0.38}$	5	0.3	158(169)
	12–15	4.2	”	$3.1\ \pm^{0.57}_{0.55}$	5	0.3	161.6(158)
	15–18	4.2	”	$3\ \pm^{1}_{0.75}$	3.5	0.3	27(19)
A3562	0–3	**4.0**	3.85	$4\ \pm^{0.26}_{0.33}$	$2.7\ \pm^{0.5}_{0.3}$	0.6	203.6(165)
	3–6	”	”	$3.56\ \pm^{0.5}_{0.35}$	$4.5\ \pm^{1.9}_{1.1}$	0.3	134(161)
	6–12	”	”	$3.65\ \pm^{0.65}_{0.5}$	$3.6\ \pm^{1.2}_{0.8}$	0.3	205.4(163)
A3560	0–3	**4.7**	4.6	$5.3\ \pm^{2.1}_{1.3}$	$2.2\ \pm^{1.5}_{0.6}$	$0.38\pm^{0.62}_{0.25}$	52.7(47)
	3–6	”	”	$4.2\ \pm^{2.5}_{1.6}$	$4.2\ \pm^{10}_{2.15}$	0.3	85(58)
	6–12	”	”	$4.1\ \pm^{2.9}_{1.8}$	$1.9\pm^{1.0}_{0.5}$	$0.25\pm^{0.65}_{0.24}$	104.4(78)

a – Use of best–fit values kT=7.5, A=0.5 (Markevitch et al. 1998) will result in no changes to Fig. 2 and Fig. 3.

Table 2: Modelling the PSPC spectra of some regions of A3571 and A3558 with an additional thermal or non–thermal component; parameters of the hot ICM were fixed at the best values as given in Table 2 except the normalization constant (emission measure) which was fitted to the data. For A3558, a second MEKAL component is added to the model, with the same elemental abundances as those of the hot phase; alternatively, a power–law model is added with its differential photon number index fixed at the value of α=1.75, corresponding to emitting electrons having the Galactic index of cosmic rays (see, e.g., Lieu et al. 1999). For A3571, the model employed was, in XSPEC language, a WABS*EDGE*(MEKAL+MEKAL). This model is only intended as a preliminary means of accounting for the observed spectral features, as a model that includes details of radiative transport and opacity is not currently available. These spectral models were also satisfactorily applied to the LECS data, showing that PSPC and LECS give consistent results.

Cluster	region (arcmin)	2^{nd} thermal comp.				2^{nd} non–thermal comp.
		T (keV)			$\Delta\chi^2$ (Δ d.o.f.)	$\Delta\chi^2$(Δ d.o.f.)
A3558	3–6	$0.04\ \pm^{0.06}_{0.02}$			15(2)	13(1)
	6–9	$0.05\ \pm^{0.1}_{0.03}$			24(2)	35(1)
		T (keV)	edge E (keV)	edge τ	$\Delta\chi^2$ (Δ d.o.f.)	
A3571	4–8	$0.85\ \pm^{0.6}_{0.2}$	$0.52\pm^{0.04}_{0.09}$	$0.98\pm^{0.65}_{0.05}$	51(4)	

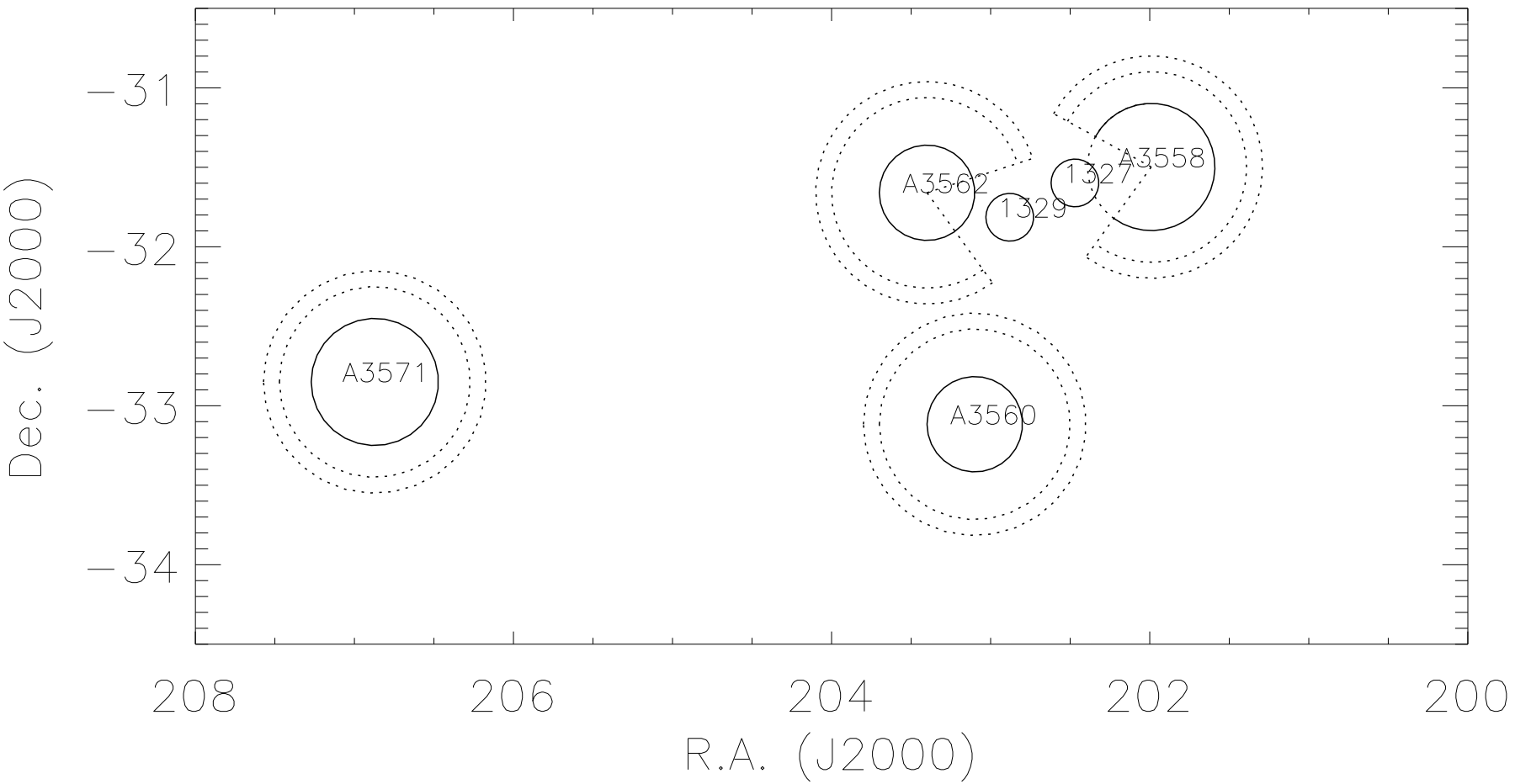
A3562
1327
A3558
1329
A3571
A3560
−31
−32
−33
−34
208
206
204
202
200
Dec. (J2000)
R.A. (J2000)

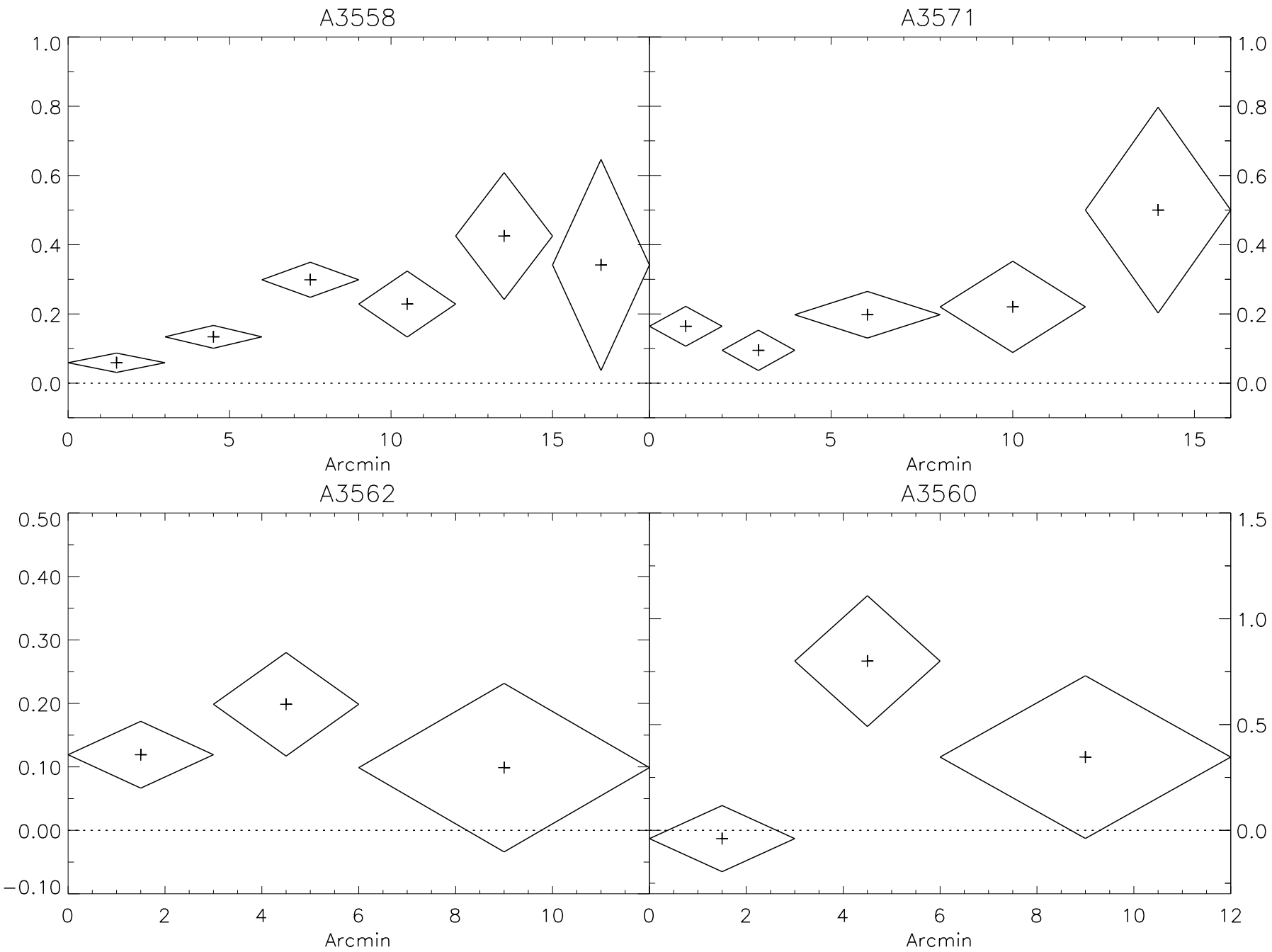
A3558
A3571
A3562
A3560
Arcmin
Arcmin
Arcmin
Arcmin

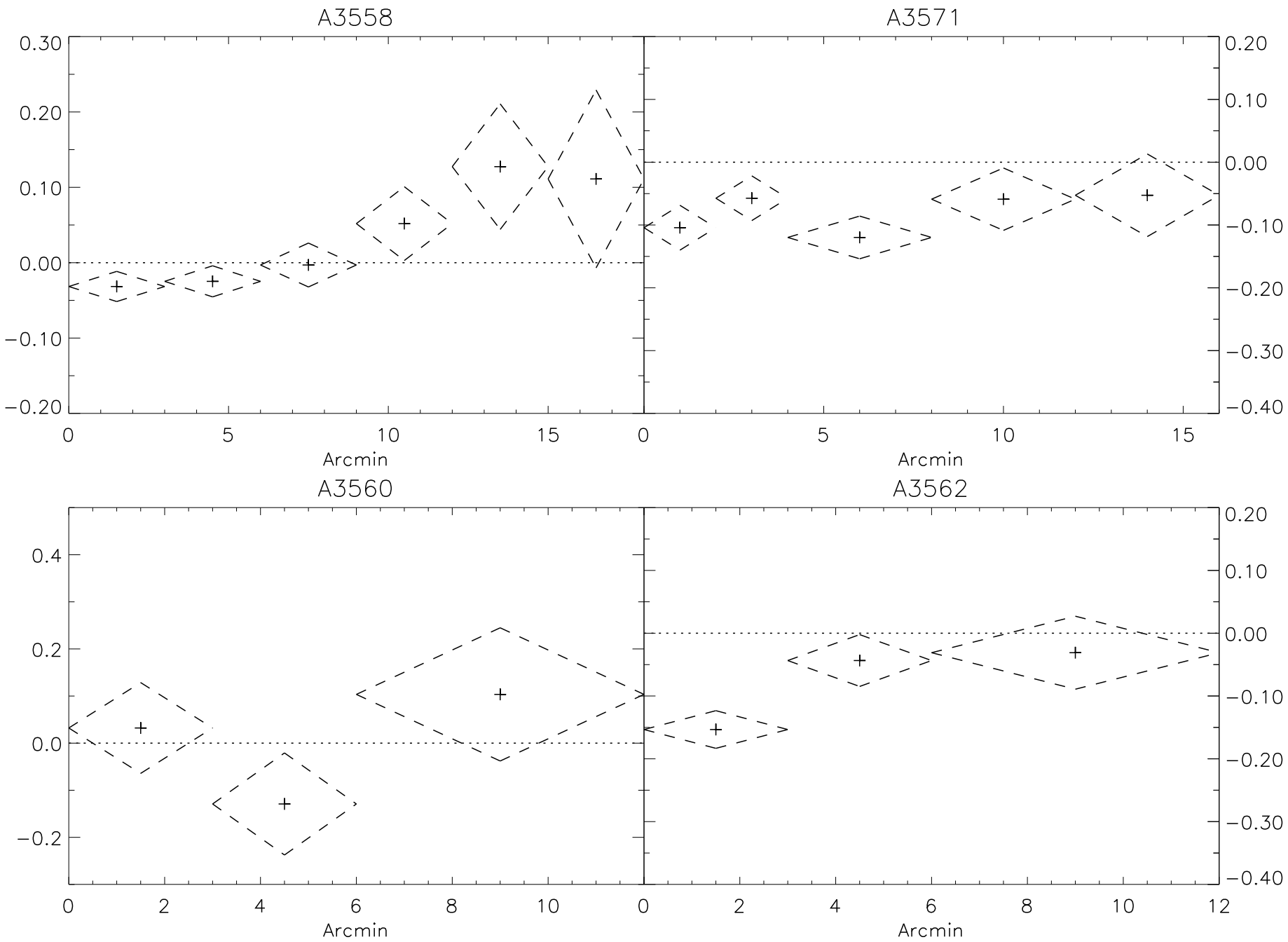
A3558
A3571
A3560
A3562
Arcmin
Arcmin
Arcmin
Arcmin

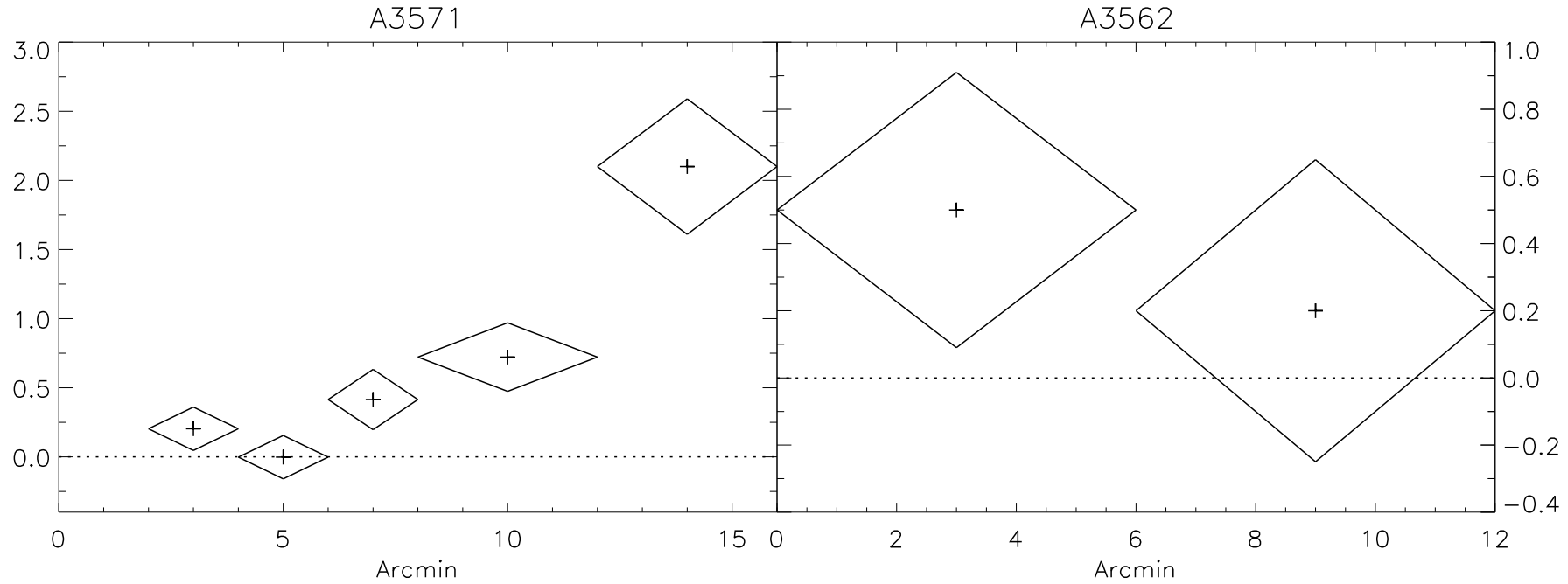
A3571
A3562
3.0
2.5
2.0
1.5
1.0
0.5
0.0
1.0
0.8
0.6
0.4
0.2
0.0
−0.2
−0.4
0
5
10
15
0
2
4
6
8
10
12
Arcmin
Arcmin

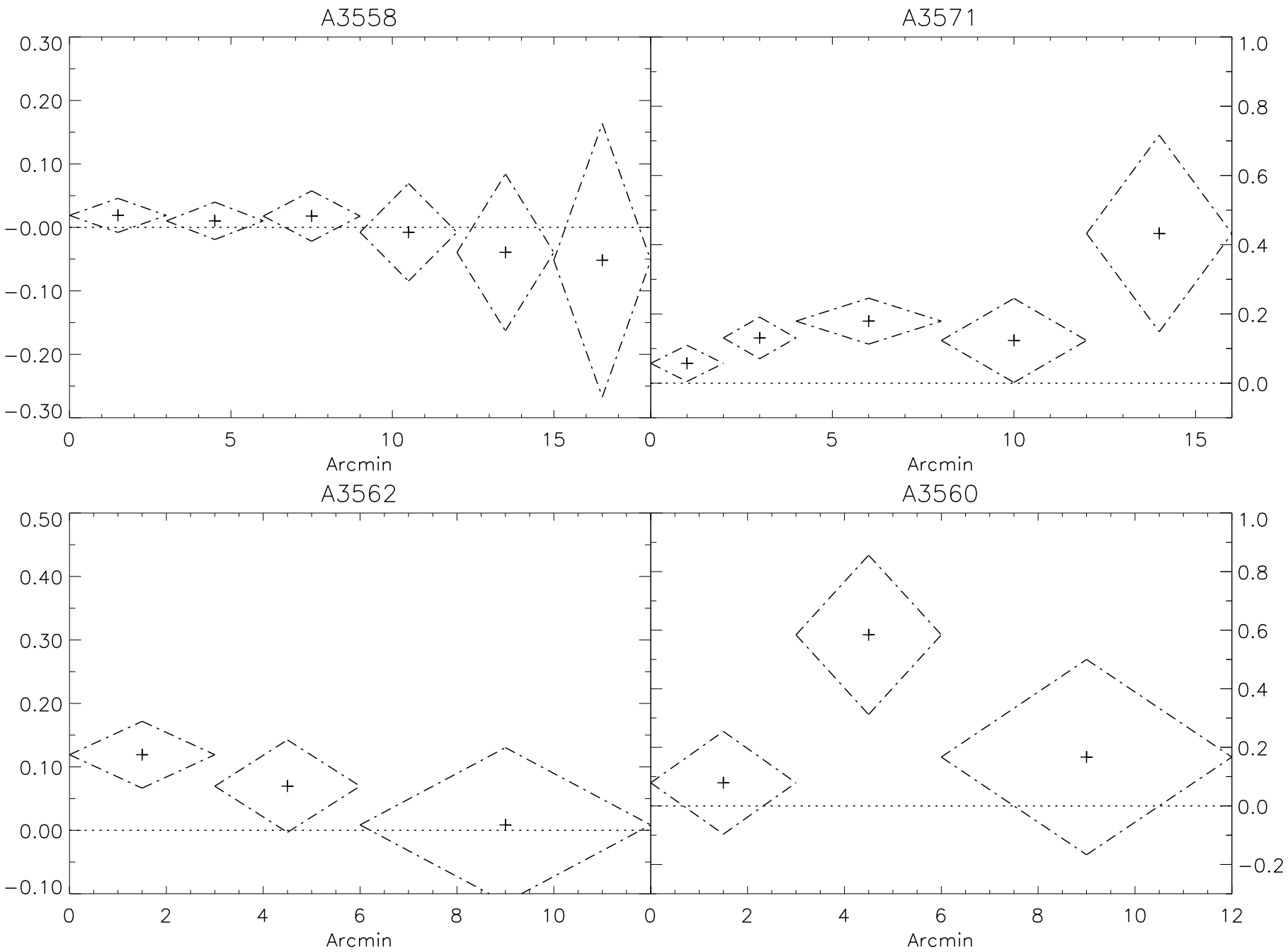
A3558
A3571
A3562
A3560
Arcmin
Arcmin
Arcmin
Arcmin